Smoothing the Payoff for Efficient Computation of Option Pricing in Time-Stepping Setting

1 Introduction

1.1 The goal and outline of the project

The first goal of the project is to approximate $\mathrm{E}[f(X(t))]$, using multi-index stochastic collocation(MISC) method, proposed in [9], where

- The payoff $f : \mathbb{R}^d \to \mathbb{R}$ has either jumps or kinks. Possible choices of f that we wanted to test are:
  - hockey-stick function, i.e., put or call payoff functions;
  - indicator functions (both relevant in finance (binary option,...) and in other applications of estimation of probabilities of certain events);
  - delta-functions for density estimation (and derivatives thereof for estimation of derivatives of the density).

  More specifically, f should be the composition of one of the above with a smooth function. (For instance, the basket option payoff as a function of the log-prices of the underlying.)
- The process X is simulated via a time-stepping scheme. Possible choices that we wanted to test are
  - The one/multi dimensional discretized Black-Scholes(BS) process where we compare different ways to identify the location of the kink, such as:
    - Exact location of the continuous problem
    - Exact location of the discrete problem by root finding of a polynomial in y.
    - Newton iteration.
  - A relative simple interest rate model or stochastic volatility model, for instance CIR or Heston models: In fact, the impact of the Brownian bridge will disappear in the limit, which may make the effect of the smoothing, but also of the errors in the kink location difficult to identify. For this reason, we suggest to study a more complicated 1-dimensional problem next. We suggest to use a CIR process. To avoid complications at the boundary, we suggest "nice" parameter choices, such that the discretized process is very unlikely to hit the boundary (Feller condition).

– The multi dimensional discretized Black-Scholes(BS) process: Here, we suggest to return to the Black-Scholes model, but in multi-dimensional case. In this case, linearizing the exponential, suggest that a good variable to use for smoothing might be the sum of the final values of the Brownian motion. In general, though, one should probably eventually identify the optimal direction(s) for smoothing via the duals algorithmic differentiation.

The desired outcome is a paper including

- Theoretical results including: i) an analiticity proof for the integrand in the time stepping setting, ii) a numerical analysis of the schemes involved, such as Newton iteration, etc.
- Applications that tests the examples above.

What has beed achieved so far:

1. Numerical outputs:
   - **Example 1**: Tests for the basket option with the smoothing trick as in [1] (see Section 5.1): in that example we checked the performance of MISC without time stepping scheme and also compare the results with reference [1]. (Done).
   -
   - **Example 2**: The one dimensional binary option under discretized BS model (see Section 5.3): We tested a simple case which is given by the binary option. We tested the weak rates (with and without using the Richardson extrapolation). The results are promising.
   - **Example 3**: The one dimensional call option under discretized BS model (see Section 5.2): In this example, we compared different ways (exact/approximate) to determine the kink (See section 5.2.1). In a second step, we tried to approximate the option price using MISC (with/without Richardson extrapolation). We observed some issues of convergence when using Richardson extrapolation, therefore, we added another case where we use a smooth payoff (with/without Richardson) and there we observed an advantage of using Richardson (see Section D). We do not have any clues why we have such problem when coupling MISC with Richardson for the non-smooth case. I provide in Section **??** some analysis that may explain why we do not see an improvement the way we are coupling MISC with Richardson extrapolation and then maybe we need to do it differently. (**Under checking**)
2. Theoretical outputs:
   - Heuristic proof of analiticity (See Section .)

1.2 Literature review

Many option pricing problems require the computation of multivariate integrals. The dimension of these integrals is determined by the number of independent stochastic factors (e.g. the number of time steps in the time discretization or the number of assets under consideration). The high dimension of these integrals can be treated with dimension-adaptive quadrature methods to have the desired convergence behavior.

Unfortunately, in many cases, the integrand contains either kinks and jumps. In fact, an option is normally considered worthless if the value falls below a predetermined strike price. A kink (discontinuity in the gradients) is present when the payoff function is continuous, while a jump (discontinuity in the function) exists when the payoff coreesponds to a binary or other digital options. The existence of kinks or jumps in the integrand heavily degrades the performance of quadrature formulas. In this work, we are interested in solving this problem by using adaptive sparse grids (SG) methods coupled with suitable transformations. The main idea is to find lines or areas of discontinuity and to employ suitable transformations of the integration domain. Then by a pre-integration (smoothing) step with respect to the dimension containing the kink/jump, we end up with integrating only over the smooth parts of the integrand and the fast convergence of the sparse grid method can be regained.

One can ignore the kinks and jumps, and apply directly a method for integration over $\mathbb{R}^d$. Despite the significant progress in SG methods [2] for high dimensional integration of smooth integrands, few works have been done to deal with cases involving integrands with kinks or jumps due to the decreasing performance of SG methods in the presence of kinks and jumps.

Some works [6, 1, 7, 8, 10] adressed similar kind of problems, characterized by the presence of kinks and jumps, but with much more emphasis on Quasi Monte Carlo (QMC). In [6, 7, 8], an analysis of the performance of Quasi Monte Carlo (QMC) and SG methods has been conducted, in the presence of kinks and jumps. In [6, 7], the authors studied the terms of the ANOVA decomposition of functions with kinks defined on d-dimensional Euclidean space $\mathbb{R}^d$, and showed that under some assumptions all but the the highest order ANOVA term of the 2^d ANOVA terms can be smooth for the case of an arithmetic Asian option with the Brownian bridge construction. Furthermore, [8] extended the work in [6, 7] from kinks to jumps for the case of an arithmetic average digital Asian option with the principal component analysis (PCA). The main findings in [6, 7] was obtained for an integrand of the form $f(\mathbf{x}) = \max(\phi(\mathbf{x}), 0)$ with ϕ being smooth. In fact, by assuming i) the d-dimensional function ϕ has a positive partial derivative with respect to x_j for some $j \in \{1, \ldots, d\}$, ii) certain growth conditions at infinity are satisfied, the authors showed that the ANOVA terms of f that do not depend on the variable x_j are smooth. We note that [6, 7, 8] focus more on theoretical aspects of applying QMC in such a setting. On the other hand, we focus more on specific practical problems, where we add the adaptivity paradigm to the picture.

A recent work [10] adresses similar kind of problems using QMC. Being very much related to [1], the authors i) assume that the conditional expectation can be computed explicitly, by imposing very strong assumptions. ii) Secondly, they use PCA on the gradients to reduce the effective dimension. In our work, we do not make such assumptions, which is why we need numerical methods, more precisely root finding and the quadrature in the first direction.

1.3 Notation

In the following, we clarify some notations that we will be using in this paper:

- Given $\mathbf{x} \in \mathbb{R}^N$, $\mid \mathbf{x} \mid_0$ denotes the number of non-zero components of $\mathbf{x}$.
- $\mathcal{L}_+$ denotes the set of sequences with positive components with only finitely many elements larger than 1, *i.e.*, $\mathcal{L}_+ = \{\boldsymbol{\beta} \in \mathbb{N}_+^{\mathbb{N}} :\mid \boldsymbol{\beta} - 1 \mid_0 < \infty\}$.

2 Problem formulation and Setting

In the context of option pricing, we aim at approximating the option price, $E[g(\mathbf{X}(t))]$, where $g : \mathbb{R}^d \to \mathbb{R}$ is the payoff function and where the process of the asset prices $\mathbf{X} \in \mathbb{R}^d$ solves

$$\mathbf{X}(t) = \mathbf{X}(0) + \int_0^t a(s, \mathbf{X}(s))ds + \sum_{\ell=1}^{\ell_0} \int_0^t b^\ell(s, \mathbf{X}(s))dW^\ell(s) \tag{1}$$

Let us denote by $\Phi : (\mathbf{z}_1, \ldots, \mathbf{z}_N) \to \mathbf{X}_T$, the mapping consisting of the time-stepping scheme, where $\{\mathbf{z}_i\}_{i=1}^N$ are independent d-dimensional Gaussian random vectors, and N is the number of time steps. Without loss of Generality, we assume that Φ may include pre-processing transformations to reduce the effective dimension. We also assume that $d = 1$ and the extension to higher dimension is trivial.

In this setting, we are interetsed in the basic problem of approximating

$$E[g(\mathbf{X}(t))] = I_N(g \circ \Phi) := \int_{\mathbb{R}^N} g \circ \Phi(\mathbf{z})d\mathbf{z} = \int_{-\infty}^{\infty} \cdots \int_{-\infty}^{\infty} g \circ \Phi(z_1, \ldots, z_N)\rho_d(\mathbf{z})dz_1, \ldots, dz_N, \tag{2}$$

with

$$\rho_N(\mathbf{z}) = \frac{1}{(2\pi)^{N/2}} e^{-\frac{1}{2}\mathbf{z}^T\mathbf{z}}. \tag{3}$$

where ρ is a continuous and strictly positive probability density function on $\mathbb{R}$ and g is a real-valued function integrable with respect to ρ_N.

In this context, we work mainly with two possible structures of payoff function g. In fact, for the cases of call/put options, the payoff g has a kink and will be of the form

$$g(\mathbf{x}) = \max(\phi(\mathbf{x}), 0). \tag{4}$$

One can also encounter jumps in the payoff when working with binary digital options. In this case, g is given by

$$g(\mathbf{x}) = \mathbf{1}_{(\phi(\mathbf{x})\geq 0)}. \tag{5}$$

We introduce the notation $\mathbf{x} = (x_j, \mathbf{x}_{-j})$, where $\mathbf{x}_{-j}$ denotes the vector of length $d-1$ denoting all the variables other than x_j. Then, if we assume for some $j \in \{1, \ldots, d\}$

$$\frac{\partial \phi}{\partial x_j}(\mathbf{x}) > 0, \ \forall \mathbf{x} \in \mathbb{R}^d \ \textbf{(Monotonicity condition)} \tag{6}$$

$$\lim_{x\to+\infty} \phi(\mathbf{x}) = \lim_{x\to+\infty} \phi(x_j, \mathbf{x}_{-j}) = +\infty, \text{ or } \frac{\partial^2 \phi}{\partial x_j^2}(\mathbf{x}) \ \textbf{(Growth condition)}, \tag{7}$$

then, using Fubini's theorem, we can rewrite (2) as

$$
\begin{aligned}
(8) \qquad I_N(g \circ \Phi) &= \int_{\mathbb{R}^{d-1}} \left(\int_{-\infty}^{\infty} g \circ \Phi(z_j, \mathbf{z}_{-j}) \rho(z_j) dz_j \right) \rho_{z-1}(\mathbf{z}_{-j}) d\mathbf{z}_{-j}, \\
&= \mathrm{E}\left[E\left[g \circ \Phi(z_j, \mathbf{z}_{-j}) \mid z_j \right] \right]
\end{aligned}
$$

where we evaluate the inner integral for each $\mathbf{z}_{-j}$ and which results in a smooth integrand for the outer $(N-1)$-dimensional integral.

We note that conditions ((6) and (7)) imply that for each $\mathbf{z}_{-j}$, the function $\phi \circ \Phi(z_j, \mathbf{z}_{-j})$ either has a simple root z_j or is positive for all $z_j \in \mathbb{R}$.

We generally do not have a closed form for the inside integral in 8. Therefore, the pre-integration (conditional sampling) step should be performed numerically.

3 Details of our approach

In the following, we describe our approach which basically can be seen as a two stage method. In the first step, we use root finding procedure to get the inside integral in 8, then in a second stage we employ adaptive quadraure, multi-index stochastic collocation (MISC), to compute the obtained smooth integrand.

For illustration purposes, let us focus on the one dimensional case, where under the risk-neutral measure, the undelying asset follows the geometric Brownian motion (GBM)

$$
(9) \qquad dX_t = rX_t dt + \sigma X_t dB_t,
$$

where r is the risk-free rate, σ is the volatility and B_t is the standard Brownian motion. The analytical solution to (9) is

$$
(10) \qquad X_t = X_0 \exp((r - \sigma^2)t + \sigma B_t).
$$

The Brownian motion B_t can be constructed either sequentially using a standard random walk construction or hierarchically using Brownian bridge (BB) construction. To make an effective use of MISC, which is badly affected by isotropy, we use the BB construction since it produces dimensions with different importance for MISC (creates anisotropy), contrary to random walk procedure for which all the dimension of the stochastic space have equal importance (isotropic). We explain the BB construction in Section 3.2. This transformation plays a role of reducing the effective dimension of the problem and as a consquence accelerating the MISC procedure by reducing the compotational cost.

Another way to reduce the dimension of the problem is by using Richardson extrapolation, explained in Section 3.3. In fact, Richardson extrapolation acts on both the bias (by reducing it) and MISC procedure by redcing the number of needed time steps, N, neeeded to achive a certain tolerance, resulting in a lower dimensional problem.

Let us denote by $\psi : (z_1, \ldots, z_N) \to (B_1, \ldots, B_N)$ the mapping of BB construction and by $\Phi : (B_1, \ldots, B_N) \to X_T$, the mapping consisting of the time-stepping scheme. Then, we can express the option price as

$$\begin{aligned} \mathrm{E}\left[g(X(T))\right] &= \mathrm{E}\left[g\left(\Phi \circ \psi\right)(z_1, \ldots, z_N)\right] \\ &= \int_{-\infty}^{\infty} \cdots \int_{-\infty}^{\infty} G(z_1, \ldots, z_N)\rho_N(\mathbf{z}) dz_1, \ldots, dz_N, \end{aligned} \tag{11}$$

where $G = g \circ \Phi \circ \psi$ and

$$\rho_N(\mathbf{z}) = \frac{1}{(2\pi)^{N/2}} e^{-\frac{1}{2}\mathbf{z}^T\mathbf{z}}. \tag{12}$$

Now, we can easily apply the procedure of pre-integration of section 2, where we can assume that the payoff function g can be either the maximum or indicator function and $\phi = \Phi \circ \psi$. The remaining ingredient is to determine with respect to which variable z_j we will integrate.

Claiming that pre-integrating with respect to z_1 is the optimal option then from (11), we have

$$\begin{aligned} \mathrm{E}\left[g(X(T))\right] &= \int_{-\infty}^{\infty} \cdots \int_{-\infty}^{\infty} G(z_1, \ldots, z_N)\rho_N(\mathbf{z}) dz_1, \ldots, dz_N \\ &= \int_{\mathbb{R}^{d-1}} \left(\int_{-\infty}^{\infty} G(z_1, \mathbf{z}_{-1})\rho(z_1) dz_1 \right) \rho_{d-1}(\mathbf{z}_{-1}) d\mathbf{z}_{-1} \\ &= \int_{\mathbb{R}^{d-1}} h(\mathbf{z}_{-1})\rho_{d-1}(\mathbf{z}_{-1}) d\mathbf{z}_{-1}, \\ &= \mathrm{E}\left[h(\mathbf{z}_1)\right] \end{aligned} \tag{13}$$

where $h(\mathbf{z}_{-1}) = \int_{-\infty}^{\infty} G(z_1, \mathbf{z}_{-1})\rho(z_1) dz_1 = E\left[G\left(z_1, \ldots, z_N\right) \mid z_1\right]$.

Since g can have a kink or jump. Computing $h(\mathbf{z}_{-1})$ in the pre-integration step should be carried carefully to not deteriorate the smoothness of h. This can be done by applying a root finding procedure and then computing the uni-variate integral by summing the terms coming from integrating in each region where g is smooth. In Sections (3.4,3.5), we explain those points.

Once we perform stage 1 procedure, we use multi-index stochastic collocation (MISC) procedure, suggested in [9], to compute the expectation $\mathrm{E}\left[h(\mathbf{z}_1)\right]$. We describe the general strategy for the multi-index construction in Section 3.1.

We have a natural error decomposition for the total error of computing the the expectation in (13), namely, $\mathcal{E}$

$$\mathcal{E} \leq \mathcal{E}_Q(TOL_{\mathrm{MISC}}, N) + \mathcal{E}_B(N), \tag{14}$$

where $\mathcal{E}_Q$ is the quadrature error, function of MISC tolerance TOL_{MISC} and N (the number of time steps) and $\mathcal{E}_B$ is the bias, function of N (the number of time steps) or $\Delta_t = \frac{T}{N}$ (size of the time grid). We provide a discussion about the different errors in Section 4.

3.1 MISC details

We focus on solving the problem of approximating the expected value of $\mathrm{E}\left[f(y)\right]$ on a tensorization of quadrature formulae over the stochastic domain, Γ. Assuming that $f(y)$ is a continuous function (analytic) over Γ. A quadrature approach is very adequate.

Let us define $\beta \leq 1$ be an integer positive value referred to as a "stochastic discretization level", and $m : \mathbb{N} \to \mathbb{N}$ be a strictly increasing function with $m(0) = 0$ and $m(1) = 1$, that we call a "level-to-nodes function". At level β, we consider a set of $m(\beta)$ distinct quadrature points in $(-\infty; \infty)$, $\mathcal{H}^{m(\beta)} = \{y_\beta^1, y_\beta^2, \ldots, y_\beta^{m(\beta)}\} \subset [-\infty, \infty]$, and a set of quadrature weights, $\mathcal{W}^{m(\beta)} = \{\omega_\beta^1, \omega_\beta^2, \ldots, \omega_\beta^{m(\beta)}\}$. We also let $C^0((-\infty, \infty))$ be the set of real-valued continuous functions over $(-\infty, \infty)$. We then define the quadrature operator as

$$Q(m(\beta)) : C^0((-\infty, \infty)) \to \mathbb{R}, \quad Q(m(\beta))[f] = \sum_{j=1}^{m(\beta)} f(y_\beta^j)\omega_\beta^j. \tag{15}$$

In the multi-variate case Γ is defined as a countable tensor product of intervals. Therefore, we define, for any definitely supported multi-index $\boldsymbol{\beta} \in \mathcal{L}_+$

$$Q^{m(\boldsymbol{\beta})} : \Gamma \to \mathbb{R}, \quad Q^{m(\boldsymbol{\beta})} = \bigotimes_{n \geq 1} Q^{m(\beta_n)}$$

where the n-th quadrature operator is understood to act only on the n-th variable of f. Practically, we obtain the value of $Q^{m(\boldsymbol{\beta})}[f]$ by considering the tensor grid $\mathcal{T}^{m(\boldsymbol{\beta})} = \times_{n \geq 1} \mathcal{H}^{m(\beta_n)}$ with cardinality $\#\mathcal{T}^{m(\boldsymbol{\beta})} = \prod_{n \geq 1} m(\beta_n)$ and computing

$$Q^{\mathcal{T}^{m(\boldsymbol{\beta})}}[f] = \sum_{j=1}^{\#\mathcal{T}^{m(\boldsymbol{\beta})}} f(\widehat{y}_j)\overline{\omega}_j$$

where $\widehat{y}_j \in \mathcal{T}^{m(\boldsymbol{\beta})}$ amd $\overline{\omega}_j$ are (infinite) products of weights of the univariate quadrature rules. We Note that it is essential in this construction that $m(1) = 1$ so that the cardinality of $\mathcal{T}^{m(\boldsymbol{\beta})}$ is finite for any $\boldsymbol{\beta} \in \mathcal{L}_+$ and $\omega_{\beta_n}^1 = 1$ whenever $n = 1$, so that all weights, $\overline{\omega}_j$, are bounded.

We mention that the quadrature points are chosen to optimize the convergence properties of the quadrature error.

A direct approximation $\mathrm{E}[f] \approx Q^{m(\boldsymbol{\beta})}[f]$ is not an appropriate option due to the well-known "curse of dimensionality" effect. We use multi-index stochastic collocation (MISC) as it was suggested in [9]. MISC as a hierarchical adaptive quadrature strategy that uses stochastic discretizations and classic sparsification approach to obtain an effective approximation scheme for $\mathrm{E}[f]$.

In our setting, we are left with a N-dimensional Gaussian random inputs, which are chosen independently, and which we use as the basis of the multi-index construction.

For a multi-index $\ell = (l_i)_{i=1}^N \in \mathbb{N}^N$, we denote by $Q_\ell^N := Q(m_\ell)$ the result of a discretized integral, using N time steps , with parameters $m_\ell := (m_{l_i})_{i=1}^N$. We further define the set of differences ΔQ_ℓ^N as follows: for a single index $1 \leq i \leq N$, let

$$\Delta_i Q_\ell^N := \begin{cases} Q^N(m_\ell) - Q^N(m'_\ell) \text{ with } m'_\ell = m_{\ell - e_i}, \text{ if } \ell_i > 0 \\ Q^N(m_\ell) \text{ otherwise} \end{cases} \tag{16}$$

where e_i denotes the ith N-dimensional unit vector. Then, ΔQ_ℓ^N is defined as

$$\Delta Q_\ell^N := \left(\prod_{i=1}^N \Delta_i \right) Q_\ell^N. \tag{17}$$

Note that $Q^N(m)$ converges to the biased option price (denoted by $Q^N(\infty)$ as $m \to \infty$. Hence, we have the telescoping property

$$Q^N(\infty) = \sum_{l_1=0}^{\infty} \cdots \sum_{l_N=0}^{\infty} \Delta Q^N_{(l_1,\ldots,l_N)} = \sum_{\ell \in \mathbb{N}^N} \Delta Q^N_\ell, \tag{18}$$

provided that $m_{l_1} \xrightarrow{l_1 \to \infty} \infty$, ..., $m_{l_N} \xrightarrow{l_N \to \infty} \infty$. The telescoping property is accompanied by a corresponding error factorization, i.e., the size of the increment ΔQ^N_ℓ can be bounded by a product of error terms depending on m_i.

We denote the computational work at level $\ell = (l_1, \ldots, l_N)$ for adding an increment ΔQ^N_ℓ in the telescoping sum by W^N_ℓ, and define the actual estimator for the quantity of interest $Q^N(\infty)$: given a set of multi-indices $\mathcal{I} \subset \mathbb{N}^N$, let

$$Q^N(\mathcal{I}) \coloneqq \sum_{\ell \in \mathcal{I}} \Delta Q^N_\ell.$$

Then the error is given by

$$\left| Q^N(\infty) - Q^N(\mathcal{I}) \right| \le \sum_{\ell \in \mathbb{N}^N \setminus \mathcal{I}} \left| \Delta Q^N_\ell \right|,$$

The construction of $\mathcal{I}$ will be done by profit thresholding, i.e., for a certain threshold value T, we add a multi-index ℓ to $\mathcal{I}$ provided that

$$\log \left(\frac{\left| \Delta Q^N_\ell \right|}{W^N_\ell} \right) \le T.$$

(Actually, we take the error estimate instead of the true error.)

3.2 Brownian bridge construction

Let us denote $\{t_i\}_{i=0}^N$ the grid of time steps, then the BB construction [5] consists of the following: given a past value B_{t_i} and a future value B_{t_k}, the value B_{t_j} (with $t_i < t_j < t_k$) can be generated according to the formula:

$$B_{t_j} = (1-\rho) B_{t_i} + \rho B_{t_k} + \sqrt{\rho(1-\rho)(k-i)\Delta t}\, z,\ z \sim \mathcal{N}(0,1), \tag{19}$$

where $\rho = \frac{j-i}{k-i}$. In particular, if N is a power of 2, then given $B_0 = 0$, BB generates the Brownian motion at times $T, T/2, T/4, 3T/4, \ldots$ according

$$\begin{aligned}
B_T &= \sqrt{T} z_1 \\
B_{T/2} &= \frac{1}{2}(B_0 + B_T) + \sqrt{T/4} z_2 = \frac{\sqrt{T}}{2} z_1 + \frac{\sqrt{T}}{2} z_2 \\
B_{T/4} &= \frac{1}{2}(B_0 + B_{T/2}) + \sqrt{T/8} z_3 = \frac{\sqrt{T}}{4} z_1 + \frac{\sqrt{T}}{4} z_2 + \sqrt{T/8} z_3 \\
&\vdots
\end{aligned} \tag{20}$$

where $\{z_j\}_{j=1}^N$ are independent standard normal variables. In BB construction given by (20), the most important values that determine the large scale structure of Brownian motion are the first components of $\mathbf{z} = (z_1, \ldots, z_N)$.

3.3 Richardson extrapolation

We recall that the Euler (often) scheme has weak order 1 so that

$$\left|\mathrm{E}\left[f(\widehat{X}_T^h)\right] - \mathrm{E}\left[f(X_T)\right]\right| \leq Ch \tag{21}$$

for some constant C, all sufficiently small h and suitably smooth f. It was shown that 21 can be improved to

$$\mathrm{E}\left[f(\widehat{X}_T^h)\right] = \mathrm{E}\left[f(X_T)\right] + ch + \mathcal{O}\left(h^2\right), \tag{22}$$

where c depends on f.
Applying 22 with discretization step $2h$, we obtain

$$\mathrm{E}\left[f(\widehat{X}_T^{2h})\right] = \mathrm{E}\left[f(X_T)\right] + 2ch + \mathcal{O}\left(h^2\right), \tag{23}$$

implying

$$2\mathrm{E}\left[f(\widehat{X}_T^{2h})\right] - \mathrm{E}\left[f(\widehat{X}_T^h)\right] = \mathrm{E}\left[f(X_T)\right] + \mathcal{O}\left(h^2\right), \tag{24}$$

For higher levels extrapolations, we use the following: Let us denote by $h_J = h_0.2^{-J}$ the grid sizes (where h_0 is the coarsest grid size), by K the level of the Richardson extrapolation, and by $I(J,K)$ the approximation of $\mathrm{E}\left[f(\widehat{X}_T^{h_J})\right]$ by terms up to level K (leading to a weak error of order K), then we have

$$I(J,K) = \frac{2^K\left[I(J,K-1) - I(J-1,K-1)\right]}{2^K - 1} + \mathcal{O}\left(h^{K+1}\right), \quad J = 1,2,\ldots, K = 1,2,\ldots \tag{25}$$

3.4 Root Finding

Without loss of generality, we can assume that the integration domain can be divided into two parts Ω_1, and Ω_2 such that the integrand f is smooth and positive in Ω_1 whereas $f(\mathbf{x}) = 0$ in Ω_2. Therefore,

$$If := \int_{\Omega_1} f(\mathbf{x}) d\mathbf{x} \tag{26}$$

This situation may arise when the integrand is non-differentiable or noncontinuous along the boundary between Ω_1 and Ω_2. For these problems, kinks and jumps can efficiently be identified by a one-dimensional root finding. Then, the kinks and jumps can be transformed to the boundary of integration domain such that they no longer deteriorate the performance of the numerical methods. In fact, we compute the zeros of the integrand with respect to the last dimension. In this dimension,

then, e.g., Newton's method or bisection can be used to identify the point which separates Ω_1 and Ω_2. In our project, we use Newton 's iteration solver.

Let us call y the mapping such that: $y : \mathbf{z}_1 \to z^{\text{kink}}$, where z^{kink} is the "location of irregularity", *i.e.*, g is not smooth at the point $\phi \circ \Phi \circ \Psi(z^{\text{kink}}, \mathbf{z}_{-1})$. Generally, there might be (for given $\mathbf{z}_{-1}$

- no solution, i.e., the integrand in the definition of $h(\mathbf{z}_{-1})$ above is smooth (*best case*);
- a unique solution;
- multiple solutions.

Generally, we need to assume that we are in the first or second case. Specifically, we need that

$$\mathbf{z}_{-1} \mapsto h(\mathbf{z}_{-1}) \text{ and } \mathbf{z}_{-1} \mapsto \widehat{h}(\mathbf{z}_{-1})$$

are smooth, where $\widehat{h}$ denotes the numerical approximation of h based on a grid containing $y(\mathbf{z}_{-1})$. In particular, y itself should be smooth in $\mathbf{z}_{-1}$. This would already be challenging in practice in the third case. Moreover, in the general situation we expect the number of solutions y to increase when the discretization of the SDE gets finer.

In many situations, case 2 (which is thought to include case 1) can be guaranteed by monotonicity (I think we need to add also the growth condition. For instance, in the case of one-dimensional SDEs with z_1 representing the terminal value of the underlying Brownian motion (and $\mathbf{z}_{-1}$ representing the Brownian bridge), this can often be seen from the SDE itself. Specifically, if each increment "dX" is increasing in z_1, no matter the value of X, then the solution X_T must be increasing in z_1. This is easily seen to be true in examples such as the Black-Scholes model and the CIR process. (Strictly speaking, we have to distinguish between the continuous and discrete time solutions. In these examples, it does not matter.) On the other hand, it is also quite simple to construct counter examples, where monotonicity fails, for instance SDEs for which the "volatility" changes sign, such as a trigonometric function.[1]

Even in multi-dimensional settings, such monotonicity conditions can hold in specific situations. For instance, in case of a basket option in a multivariate Black Scholes framework, we can choose a linear combination z_1 of the terminal values of the driving Bm, such that the basket is a monotone function of z_1. (The coefficients of the linear combination will depend on the correlations and the weights of the basket.) However, in that case this may actually not correspond to the optimal "rotation" in terms of optimizing the smoothing effect.

3.5 Description of the Domain Decomposition and Suitable Transformation

The payoff function is not smooth due to the nature of the option. In fact, the holder would not exercise the option if a purchase or sale of the underlying asset would lead to a loss. As a result, the discontinuity of the payoff function carries over to the integrand. In this case, The integrand shows a kink or even a jump with respect to a manifold. Since some (mixed) derivatives are not bounded at these manifolds, the smoothness requirements for the sparse grid method are clearly not fulfilled any more.

[1] Actually, in every such case the simple remedy is to replace the volatility by its absolute value, which does not change the law of the solution. Hence, there does not seem to be a one-dimensional counter-example.

The first step consists of identifying the areas of discontinuity or non-differentiability. Then, we decompose the total integration domain Ω into sub-domains Ω_i, $i = 1, \ldots, n$ such that the integrand is smooth in the interior of Ω_i and such that all kinks and jumps are located along the boundary of these areas. This procedure results in integrating several smooth functions, instead of one discontinuous function. The total integral is then given as the sum of the separate integrals, *i.e.*

$$If := \int_\Omega f(\mathbf{x}) d\mathbf{x} = \sum_{i=1}^{n} \int_{\Omega_i} f(\mathbf{x}) d\mathbf{x} \tag{27}$$

In this way, the fast convergence of SG can be regained whereas the costs only increase by a constant (the number of terms in the sum), provided the cost required for the decomposition is sufficiently small such that it can be neglected.

In general, such a decomposition is even more expensive than to integrate the function. Nevertheless, for some problem classes, the areas of discontinuity have a particular simple form, which allows to decompose the integration domain with costs that are much smaller than the benefit which results from the decomposition. In this work, we consider those cases.

In the literature, there two classes that have been tackled. In the first one, we have the information that the kinks are part of the integration domain where the integrand is zero and can thus be identified by root finding as proposed in [3].

In the second class, we have the information that the discontinuities are located on hyperplanes, which allows a decomposition first into polyhedrons and then into orthants as discussed in [4]. In this work, we start by the first class of problems.

4 Error discussion

4.1 Errors in smoothing

For the analysis it is useful to assume that $\widehat{h}$ is a smooth function of $\mathbf{z}_{-1}$, but in reality this is not going to be true. Specifically, if the true location y of the non-smoothness in the system were available, we could actually guarantee $\widehat{h}$ to be smooth, for instance by choosing

$$\widehat{h}(\mathbf{z}_{-1}) = \sum_{k=-K}^{K} \eta_k g\left(\phi \circ \Phi \circ \Psi\left(\zeta_k(y(\mathbf{z}_{-1})), \mathbf{z}_{-1}\right)\right),$$

for points $\zeta_k \in \mathbb{R}$ with $\zeta_0 = y$ and corresponding weights η_k.[2] However, in reality we have to numerical approximate y by $\overline{y}$ with error $|y - \overline{y}| \leq \delta$. Now, the actual integrand in $\mathbf{z}_{-1}$ becomes

$$\overline{h}(\mathbf{z}_{-1}) \coloneqq \sum_{k=-K}^{K} \eta_k g\left(\phi \circ \Phi \circ \Psi\left(\zeta_k(\overline{y}(\mathbf{z}_{-1})), \mathbf{z}_{-1}\right)\right),$$

which we cannot assume to be smooth anymore. On the other hand, if $\zeta_k(y)$ is a continuous function of y and y and $\overline{y}$ are continuous in $\mathbf{z}_{-1}$, then *eventually* we will have

$$\left\|\widehat{h} - \overline{h}\right\|_\infty \leq \mathrm{TOL}, \quad \left\|h - \overline{h}\right\|_\infty \leq \mathrm{TOL},$$

[2] Of course, the points ζ_k have to be chosen in a systematic manner depending on y.

i.e., the smooth functions h and $\widehat{h}$ are close to the integrand $\overline{h}$. (Of course, this may depend on us choosing a good enough quadrature ζ!)

Remark 4.1. If the adaptive collocation used for computing the integral of $\overline{h}$ depends on derivatives (or difference quotients) of its integrand $\overline{h}$, then we may also need to make sure that derivatives of $\overline{h}$ are close enough to derivatives of $\widehat{h}$ or h. This may require higher order solution methods for determining y.

Remark 4.2. In some important cases, f may be trivial (e.g., $\equiv 0$). In these cases, we may be able to make sure that $\overline{y}$ never crosses the "location of non-smoothness". Then even $\overline{h}$ is smooth.

Remark 4.3. We expect that the global error of our procedure will be bounded by the weak error which is in our case of order $O(\Delta t)$. In this case, the overall complexity of our procedure will be of order $O(TOL^{-1})$. We note that this rate can be improved up to $O(TOL^{-\frac{1}{2}})$ if we use **Richardson extrapolation**. Another way that can improve the complexity could be based on **Cubature on Wiener Space** (This is left for a future work). The aimed complexity rate illustrates the contribution of our procedure which outperforms Monte Carlo forward Euler (MC-FE) and multi-level MC-FE, having complexity rates of order $O(TOL^{-3})$ and $O(TOL^{-2}log(TOL)^2)$ respectively.

Remark 4.4.

We need to check the impact of the error caused by the Newton iteration on the integration error. In the worst case, we expect that if the error in the Newton iteration is of order $O(\epsilon)$ than the integration error will be of order $\log(\epsilon)$. But we need to check that too.

4.2 Discussion about the Bias

4.3 Discussion about the Quadrature error

5 Numerical examples

5.1 The basket option with the smoothing trick as in [1]

The first experiment that we consider is the pricing of a European basket call option in a Black-Scholes model. The basket is composed of d assets ($d = 3, 8, 25$) and we use the same trick of smoothing the integrand that was proposed in [1]. In this case, the dimension of the parameter space $N = d - 1$. The interpolation over the parameter space is based on the tensorized Lagrangian interpolation technique with Gaussian points.

5.1.1 Results using MISC

In table 1, we summarize the observed complexity rates for different tested settings for the basket example. From this table, we can check that even with the 25 dimensional case, the complexity rate in terms of the elapsed time is at least order 1, which is better than MC, which is 2. Detailed plots for each case are given by figures (1, 2) for $d = 3$, figures (3, 4) for $d = 8$ and figures (5, 6) for $d = 25$. Mainly, from the plots, we checked that we achive the prescribed tolerance using MISC, the convergence rates of mixed differences which is a basic assumption for using MISC (we observe exponential decay of error rates wrt to the number of quadrature points) and finally the complexity rates.

# assets \	3	8	25
rate	$-1/3$	$-9/20$	$-16/25$

Table 1: Complexity rates of the different experiments for the basket option using BS model

Case of 3-dimensional Basket

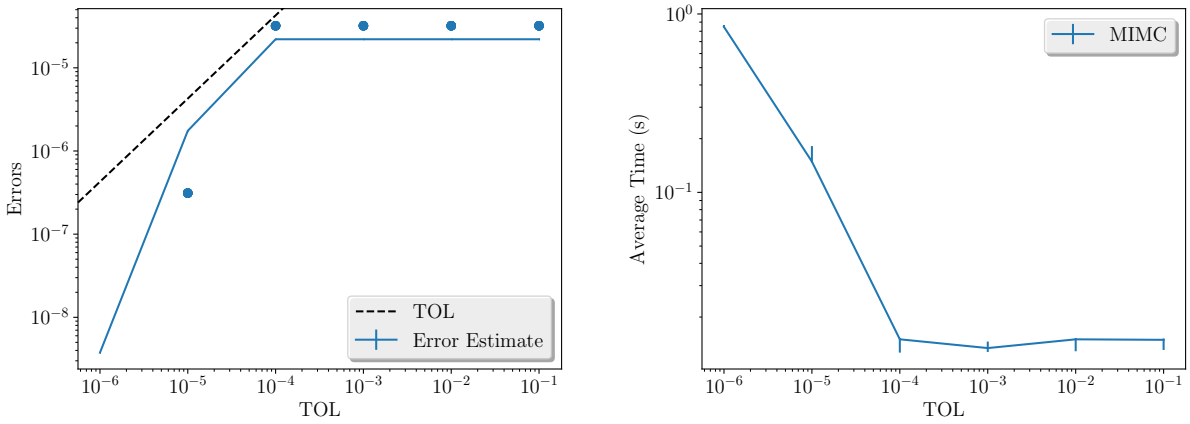

(a) Error estimate (b) Average running time as a function of TOL

Figure 1: Convergence and complexity results for the 3-dimensional basket option using BS model.

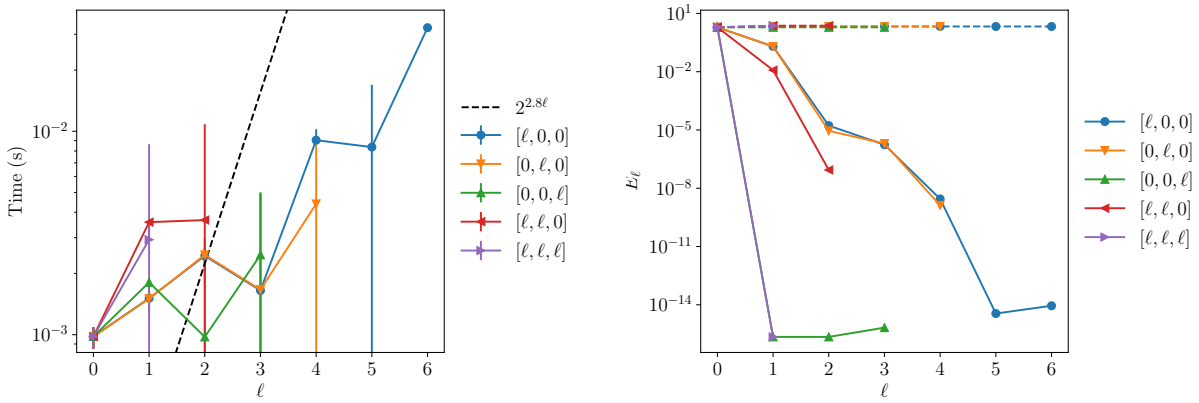

(a) Average Computational time per level. (b) The convergence rate of mixed differences per level.

Figure 2: Convergence and work rates for discretization levels for the 3-dimensional basket option using BS model.

Case of 8-dimensional Basket

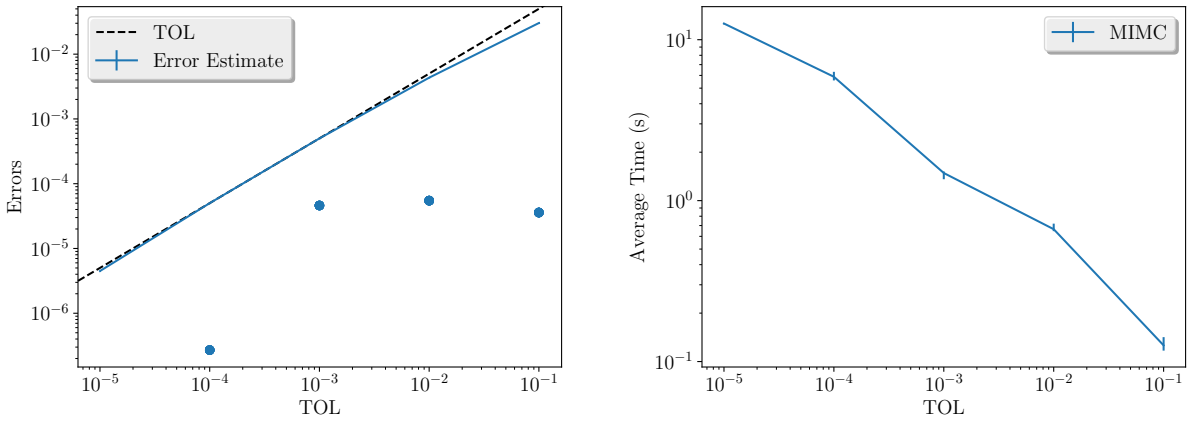

(a) Error estimate (b) Average running time as a function of TOL

Figure 3: Convergence and complexity results for the 8-dimensional basket option using BS model.

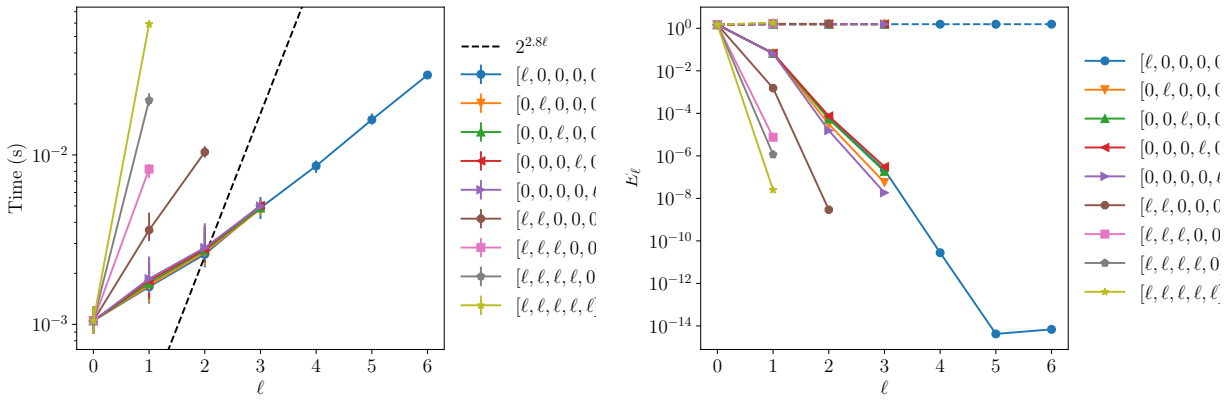

(a) Average Computational time per level. (b) The convergence rate of mixed differences per level.

Figure 4: Convergence and work rates for discretization levels for the 8-dimensional basket option using BS model.

Case of 25-dimensional Basket

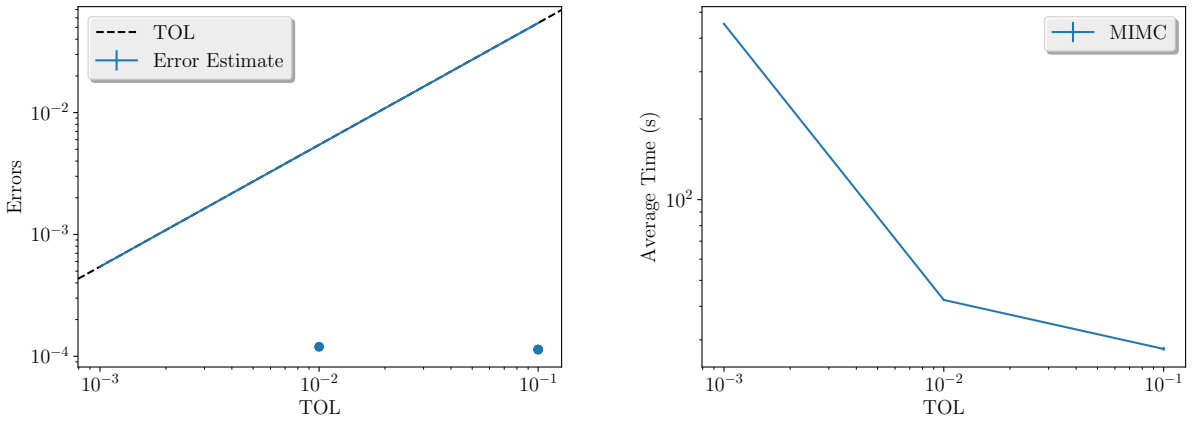

(a) Error estimate (b) Average running time as a function of TOL

Figure 5: Convergence and complexity results for the 25-dimensional basket option using BS model.

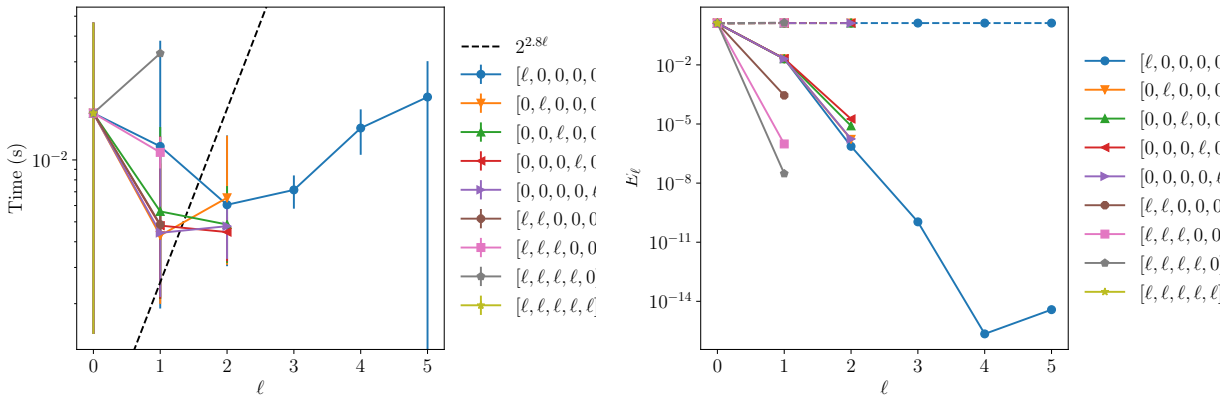

(a) Average Computational time per level. (b) The convergence rate of mixed differences per level.

Figure 6: Convergence and work rates for discretization levels for the 25-dimensional basket option using BS model.

5.2 The discretized 1D Black-Scholes

The second example that we test is the binary and call options under BS model where the process X is the discretized 1D Black-Scholes model and the payoff function g is the indicator or maximum function, and which has a kink. Precisely, we are interested in the 1-D lognormal example where the dynamics of the stock are given by

$$dX_t = \sigma X_t dW_t. \tag{28}$$

Assume that $\{W_t, 0 \leq t \leq T\}$ is a standard one-dimensional Brownian motion, and $(z_1, \ldots, z_N)$ are standard gaussian random variables, then, in the discrete case, we have

$$\begin{aligned} \Delta W_i &= (B_{t_{i+1}} - B_{t_i}) + \Delta t \frac{z_1}{\sqrt{T}} \\ &= \Delta B_i + \Delta t \frac{z_1}{\sqrt{T}}, \end{aligned} \tag{29}$$

implying that the numerical approximation of $X(T)$ satisfies

$$\begin{aligned} \overline{X}_T &= \Phi(\Delta t, z_1, \Delta B_0, \ldots, \Delta B_{N-1}), \\ &= \Phi(\Delta t, \Psi(z_1, \ldots, z_N)) \end{aligned} \tag{30}$$

for some path function Φ and Brwonian bridge map Ψ as described in Section 3.2.

As explained in Section 3, the first step of our approach is determining the location of irregularity (kink). In the following, we want to compare different ways for identifying the location of the kink for this model.

5.2.1 Determining the kink location

Exact location of the kink for the continuous problem

Let us denote y_* an invertible function that satisfies

$$X(T; y_*(x), B) = x. \tag{31}$$

We can easily prove that the expression of y_* for model given by (28) is given by

$$y_*(x) = \left(\log(x/x_0) + T\sigma^2/2\right) \frac{1}{\sqrt{T}\sigma}, \tag{32}$$

and since the kink for Black-Scholes model occurs at $x = K$, where K is the strike price then the exact location of the continuous problem is given by

$$y_*(K) = \left(\log(K/x_0) + T\sigma^2/2\right) \frac{1}{\sqrt{T}\sigma}. \tag{33}$$

Exact location of the kink for the discrete problem

The discrete problem of model (28) is solved by simulating

$$\begin{aligned} \Delta X_{t_i} &= \sigma X_{t_i} \Delta W_i, \; 0 \leq i \leq N-1 \\ X_{t_{i+1}} - X_{t_i} &= \sigma X_{t_i} \left(W_{t_{i+1}} - W_{t_i}\right), \; 0 < i < N \end{aligned} \tag{34}$$

where $X(T_0) = X_0$ and $X(t_N) = X(T)$.

Using Brownian bridge construction given by (29), we have

$$
\begin{aligned}
X_{t_1} &= X_{t_0}\left[1+\frac{\sigma}{\sqrt{T}}z_1\Delta t+\sigma\Delta B_0\right] = X_{t_0}\left[1+\sigma\Delta W_0\right]\\
X_{t_2} &= X_{t_1}\left[1+\frac{\sigma}{\sqrt{T}}z_1\Delta t+\sigma\Delta B_1\right] = X_{t_1}\left[1+\sigma\Delta W_1\right]\\
&\vdots = \vdots = \vdots\\
X_{t_N} &= X_{t_{N-1}}\left[1+\frac{\sigma}{\sqrt{T}}z_1\Delta t+\sigma\Delta B_{N-1}\right] = X_{t_{N-1}}\left[1+\sigma\Delta W_{N-1}\right], \qquad (35)
\end{aligned}
$$

implying that

$$
\overline{X}(T) = X_0\prod_{i=0}^{N-1}\left[1+\frac{\sigma}{\sqrt{T}}z_1\Delta t+\sigma\Delta B_i\right]. \qquad (36)
$$

Therefore, in order to determine y_*, we need to solve

$$
x = \overline{X}(T;y_*,B) = X_0\prod_{i=0}^{N-1}\left[1+\frac{\sigma}{\sqrt{T}}y_*(x)\Delta t+\sigma\Delta B_i\right], \qquad (37)
$$

which implies that the location of the kink point for the approximate problem is equivalent to finding the roots of the polynomial $P(y_*(K))$, given by

$$
P(y_*(K)) = \prod_{i=0}^{N-1}\left[1+\frac{\sigma}{\sqrt{T}}y_*(K)\Delta t+\sigma\Delta B_i\right]-\frac{K}{X_0}. \qquad (38)
$$

The exact location of the kink can be obtained exactly by solving exactly $P(y_*(K))=0$.

Approximate location of the discrete problem

Here, we try to find the roots of polynomial $P(y_*(K))$, given by (38), by using **Newton iteration method**. In this case, we need the expression $P' = \frac{dP}{dy_*}$. If we denote $f_i(y) = 1+\frac{\sigma}{\sqrt{T}}y\Delta t+\sigma\Delta B_i$, then we can easily show that

$$
P'(y) = \frac{\sigma\Delta t}{\sqrt{T}}\left(\prod_{i=0}^{N-1}f_i(y)\right)\left[\sum_{i=0}^{N-1}\frac{1}{f_i(y)}\right] \qquad (39)
$$

5.3 Results for the binary option example

In this case, the integrand $h(\mathbf{z}_{-1})$ is given by

$$
\begin{aligned}
h(\mathbf{z}_{-1}) &= \int \mathbf{1}_{\Phi\circ\Psi(T;z_1,\mathbf{z}_{-1})>K}\frac{1}{\sqrt{2\pi}}\exp(-z_1^2/2)dy\\
&= P(Y>y_*(K)), \qquad (40)
\end{aligned}
$$

where $y_*(x)$, is an invertible function that satisfies

$$\Phi \circ \Psi(T; y_*(x), \mathbf{z}_{-1}) = x \tag{41}$$

We get the kink point by running Newton iteration with a precision of 10^{-10}.

The paramters that we used in our numerical experiments are: $T = 1$, $\sigma = 0.4$ and $S_0 = K = 100$. The exact value of this case is 0.42074.

5.3.1 Comparing relative errors

In the following, we compare the relative errors for the binary option example under Black-Scholes model (see Tables (2, 5)). We report the results for 2 scenarios: i) Without using Richardson extrapolation, ii) Using level 1 Richardson extrapoaltion. You may see appendix A for the values of binary option prices.

Given the normalized bias computed by MC method (See Section 5.3.2) (reported as bold values in the tables), we report in red in each table the smallest tolerance that MISC required to get below that relative bias (I do not put values for smaller tolerances, once the required bias is reached).

From the tables (2, 5)), we may observe that to get a relative error below 1%, we need around 16 time steps for the case without Richardson extrapolation compared to only using 1 time step in the coarse level for the case of level 1 Richardson extraplation.

Method \Steps	2	4	8	16
MISC ($TOl = 5.10^{-1}$)	0.0982	0.0468	0.0219	0.0102
MC method ($M = 10^6$)	**0.0999**	**0.0470**	**0.0224**	**0.0099**

Table 2: Relative error of the binary option price of the different tolerances for different number of time steps, without Richardson extrapolation

Method \Steps	$1-2$	$2-4$	$4-8$	$8-16$
MISC ($TOl = 5.10^{-1}$)	0.0076	0.0045	0.0031	0.0017
MISC ($TOl = 10^{-2}$)	–	0.0036	0.0031	0.0014
MISC ($TOl = 10^{-3}$)	–	–	0.0021	0.0005
MC method ($M = 10^6$)	**0.0073**	**0.0038**	**0.0022**	**0.0006**

Table 3: Relative error of the binary option price of the different tolerances for different number of time steps, using Richardson extrapolation (level 1)

5.3.2 Weak error plots

From figure 7, we see that we get a weak error of order Δt. From figure 8, we observe an improvement in the rate and the constant when using level 1 of Richardson extrapolation. The upper and lower bounds are 95% confidence interval.

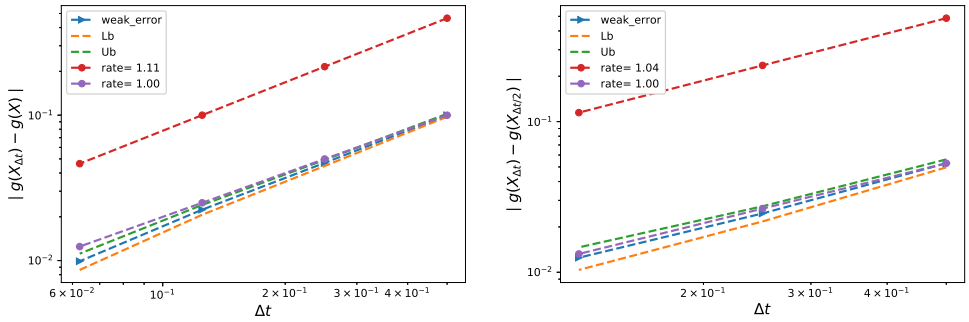

(a) (b)

Figure 7: The rate of convergence of the weak error for the binary option, without Richardson extraploation, using MC with $M = 10^4$: a) $|\mathrm{E}\left[g(X_{\Delta t})\right] - g(X)|$ b) $\left|\mathrm{E}\left[g(X_{\Delta t}) - g(X_{\Delta t/2})\right]\right|$

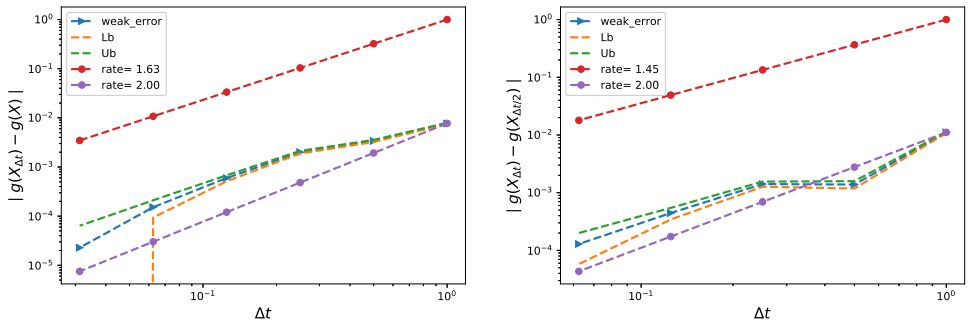

(a) (b)

Figure 8: The rate of convergence of the weak error for the binary option, with Richardson extraploation (level 1), using MC with $M = 10^6$: a) $\left|\mathrm{E}\left[2g(X_{\Delta t/2}) - g(X_{\Delta t})\right] - g(X)\right|$ b) $\left|\mathrm{E}\left[3g(X_{\Delta t/2}) - g(X_{\Delta t}) - 2g(X_{\Delta t/4})\right]\right|$

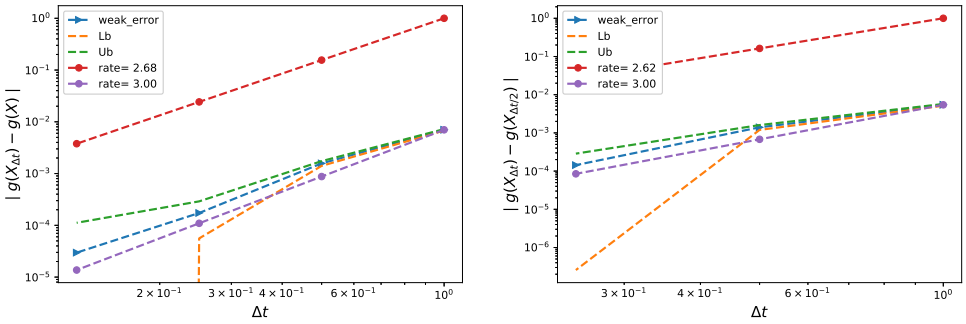

(a) (b)

Figure 9: The rate of convergence of the weak error for the binary option, with Richardson extraploation (level 2), using MC with $M = 5.10^6$: a) $\left|\frac{1}{3}\mathrm{E}\left[8g(X_{\Delta t/4}) - 6g(X_{\Delta t/2}) + g(X_{\Delta t})\right] - g(X)\right|$ b) $\left|\frac{1}{3}\mathrm{E}\left[-8g(X_{\Delta t/8}) + 14g(X_{\Delta t/4}) - 7(X_{\Delta t/2}) + g(X_{\Delta t})\right]\right|$

5.4 Results for the Call option example

In this case, the integrand $h(\mathbf{z}_{-1})$ is given by

$$h(\mathbf{z}_{-1}) = \int_{\Omega} \max\left(\Phi \circ \Psi(T; z_1, \mathbf{z}_{-1}) - K, 0\right) \frac{1}{\sqrt{2\pi}} \exp(-z_1^2/2) dy \tag{42}$$

We get the kink point by running Newton iteration with a precision of 10^{-10}. We decompose the total integration domain Ω into sub-domains Ω_i, $i = 1, 2$ such that the integrand is smooth in the interior of Ω_i and such that the kink is located along the boundary of these areas. The total integral is then given as the sum of the separate integrals, *i.e.*

$$\begin{aligned} h(\mathbf{z}_{-1}) &:= \int_{\Omega} \max\left(\Phi \circ \Psi(T; z_1, \mathbf{z}_{-1}) - K, 0\right) \frac{1}{\sqrt{2\pi}} \exp(-z_1^2/2) dy \\ &= \sum_{i=1}^{2} \int_{\Omega_i} \max\left(\Phi \circ \Psi(T; z_1, \mathbf{z}_{-1}) - K, 0\right) \frac{1}{\sqrt{2\pi}} \exp(-z_1^2/2) dy, \end{aligned} \tag{43}$$

where we use Gauss-laguerre quadrature with β points to get each part.

The paramters that we used in our numerical experiments are: $T = 1$, $\sigma = 0.4$ and $S_0 = K = 100$. The exact value of this case is 15.8519.

5.4.1 Comparing relative errors

In the following, we compare the relative errors for the call option example under Black-Scholes model(see Tables (4, 5, 6)). We report the results for 3 scenarios: i) Without using Richardson extrapolation, ii) Using level 1 Richardson extrapoaltion, iii) Using level 2 Richardson extrapoaltion. You may see appendix B for the values of call option prices. The value of β used to get those points is $\beta = 10$.

Given the normalized bias computed by MC method (See Section 5.4.2) (reported as bold values in the tables), we report in red in each table the smallest tolerance that MISC required to get below that relative bias (I do not put values for smaller tolerances, once the required bias is reached). In case I do not reach those bias I put the best value that I get with MISC in red.

From the tables (4, 5, 6)), we may observe that to get a relative error below 0.5%, we need more than 16 time steps for the case without Richardson extrapolation compared to only using 4 time step in the coarse level for the case of level 1 Richardson extraplation, and only using 1 time step in the coarse level for the case of level 2 Richardson extraplation.

Method \Steps	2	4	8	16
MISC ($TOl = 5.10^{-1}$)	0.0229	0.0179	0.0111	0.0068
MISC ($TOl = 10^{-3}$)	–	0.0177	–	0.0066
MC method ($M = 10^5$)	**0.0231**	**0.0175**	**0.0111**	**0.0064**

Table 4: Relative error of the call option price of the different tolerances for different number of time steps, without Richardson extrapolation

Method \Steps	$1-2$	$2-4$	$4-8$	$8-16$
MISC ($TOl = 5.10^{-1}$)	0.0372	0.0129	0.0043	0.0025
MISC ($TOl = 10^{-3}$)	–	0.0126	0.0042	0.0023
MC method ($M = 10^5$)	**0.0374**	**0.0116**	**0.0027**	**0.0022**

Table 5: Relative error of the call option price of the different tolerances for different number of time steps, using Richardson extrapolation (level 1)

Method \Steps	$1-2-4$	$2-4-8$	$4-8-16$
MISC ($TOl = 5.10^{-1}$)	0.0047	0.0015	0.0019
MISC ($TOl = 10^{-3}$)	0.0043	0.0013	0.0017
MC method ($M = 10^6$)	**0.0041**	**0.0013**	**0.0016**

Table 6: Relative error of the call option price of the different tolerances for different number of time steps, using Richardson extrapolation (level 2)

5.4.2 Weak error plots

In this Section, we provide the weak rate plots, for the call option for two cases: $\beta = 10$ and $\beta = 32$ (β: the number of quadrature points used for Laguere to get $h(\mathbf{z}_{-1})$). We may clearly notice that we observe the right behavior of the weak error as we kill the laguerre quadrature error by increasing β.

$\beta = 10$

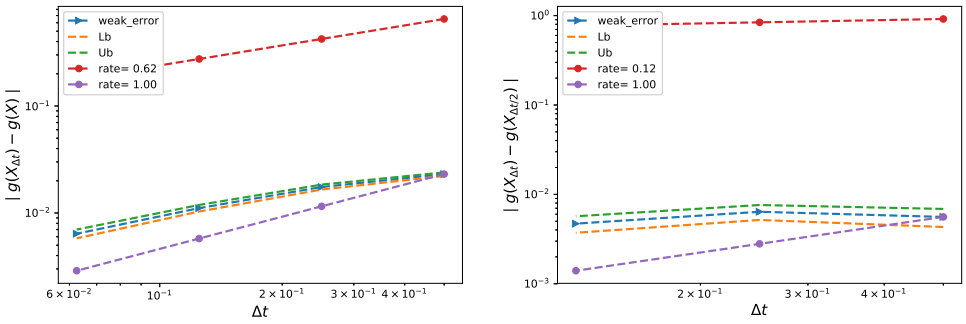

(a) (b)

Figure 10: The rate of convergence of the weak error for the call option, without Richardson extraploation, using MC with $M = 10^5$: a) $|\mathrm{E}\left[g(X_{\Delta t})\right] - g(X)|$ b) $\left|\mathrm{E}\left[g(X_{\Delta t}) - g(X_{\Delta t/2})\right]\right|$

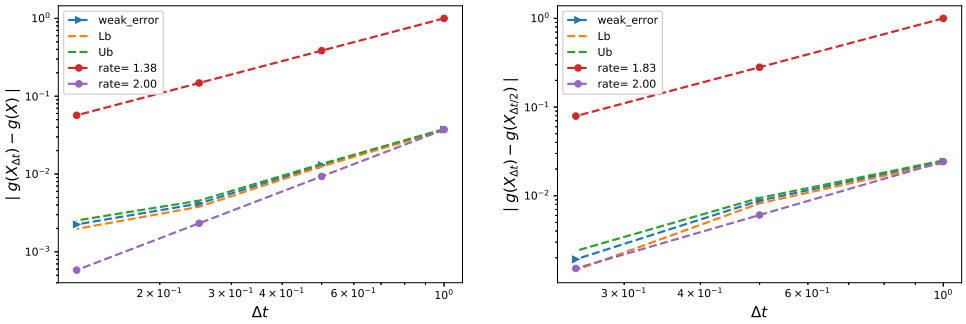

(a) (b)

Figure 11: The rate of convergence of the weak error for the call option with Richardson extraploation, using MC with $M = 10^6$: a) $\left|\mathrm{E}\left[2g(X_{\Delta t/2}) - g(X_{\Delta t})\right] - g(X)\right|$ b) $\left|\mathrm{E}\left[3g(X_{\Delta t/2}) - g(X_{\Delta t}) - 2g(X_{\Delta t/4})\right]\right|$

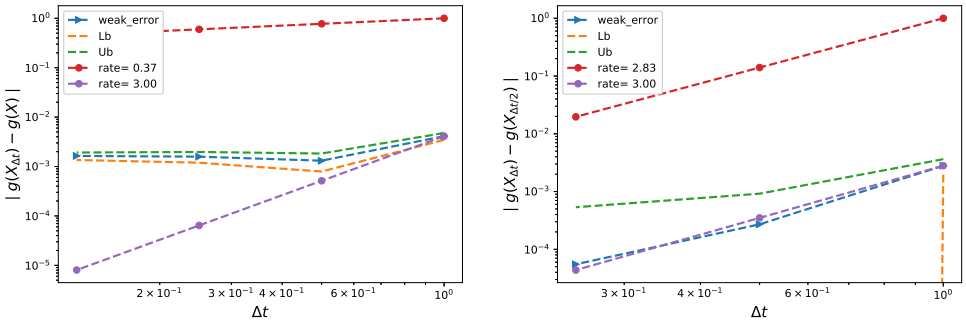

(a) (b)

Figure 12: The rate of convergence of the weak error for the call option with Richardson extraploation (level 2), using MC with $M = 10^6$: a) $\left|\frac{1}{3}\mathrm{E}\left[8g(X_{\Delta t/4}) - 6g(X_{\Delta t/2}) + g(X_{\Delta t})\right] - g(X)\right|$ b) $\left|\frac{1}{3}\mathrm{E}\left[-8g(X_{\Delta t/8}) + 14g(X_{\Delta t/4}) - 7(X_{\Delta t/2}) + g(X_{\Delta t})\right]\right|$

$\beta = 32$

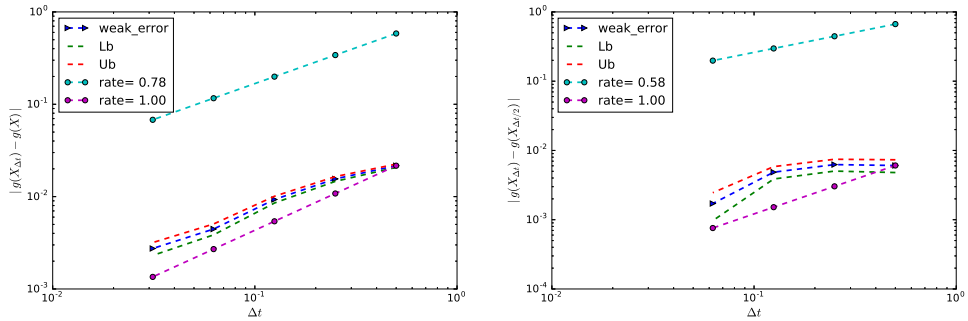

(a) (b)

Figure 13: The rate of convergence of the weak error for the call option, without Richardson extraploation, using MC with $M = 10^5$: a) $|\mathrm{E}\left[g(X_{\Delta t})\right] - g(X)|$ b) $\left|\mathrm{E}\left[g(X_{\Delta t}) - g(X_{\Delta t/2})\right]\right|$

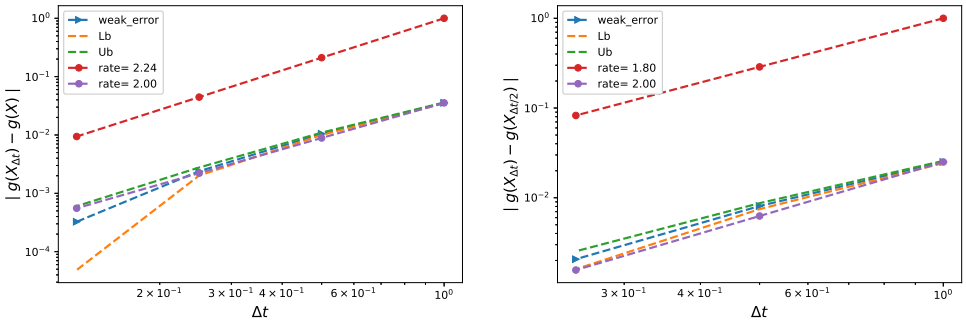

(a) (b)

Figure 14: The rate of convergence of the weak error for the call option with Richardson extraploation (level 1), using MC with $M = 5.10^6$: a) $\left|\mathrm{E}\left[2g(X_{\Delta t/2}) - g(X_{\Delta t})\right] - g(X)\right|$ b) $\left|\mathrm{E}\left[3g(X_{\Delta t/2}) - g(X_{\Delta t}) - 2g(X_{\Delta t/4})\right]\right|$

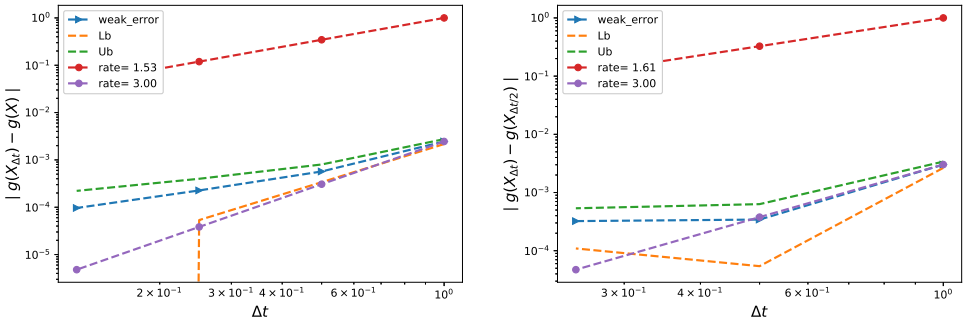

(a) (b)

Figure 15: The rate of convergence of the weak error for the call option with Richardson extraploation (level 2), using MC with $M = 5.10^6$: a) $\left|\frac{1}{3}\mathrm{E}\left[8g(X_{\Delta t/4}) - 6g(X_{\Delta t/2}) + g(X_{\Delta t})\right] - g(X)\right|$ b) $\left|\frac{1}{3}\mathrm{E}\left[-8g(X_{\Delta t/8}) + 14g(X_{\Delta t/4}) - 7(X_{\Delta t/2}) + g(X_{\Delta t})\right]\right|$

References Cited

[1] CHRISTIAN BAYER, MARKUS SIEBENMORGEN, and RAUL TEMPONE. Smoothing the payoff for efficient computation of basket option pricing.

[2] Hans-Joachim Bungartz and Michael Griebel. Sparse grids. *Acta numerica*, 13:147–269, 2004.

[3] Thomas Gerstner. Sparse grid quadrature methods for computational finance.

[4] Thomas Gerstner and Markus Holtz. Valuation of performance-dependent options. *Applied Mathematical Finance*, 15(1):1–20, 2008.

[5] Paul Glasserman. *Monte Carlo methods in financial engineering*. Springer, New York, 2004.

[6] Michael Griebel, Frances Kuo, and Ian Sloan. The smoothing effect of integration in ˆ{} and the anova decomposition. *Mathematics of Computation*, 82(281):383–400, 2013.

[7] Michael Griebel, Frances Kuo, and Ian Sloan. Note on the smoothing effect of integration in ˆ{} and the anova decomposition. *Mathematics of Computation*, 86(306):1847–1854, 2017.

[8] Andreas Griewank, Frances Y Kuo, Hernan Leövey, and Ian H Sloan. High dimensional integration of kinks and jumps–smoothing by preintegration. *arXiv preprint arXiv:1712.00920*, 2017.

[9] Abdul-Lateef Haji-Ali, Fabio Nobile, Lorenzo Tamellini, and Raul Tempone. Multi-index stochastic collocation for random pdes. *Computer Methods in Applied Mechanics and Engineering*, 306:95–122, 2016.

[10] Ye Xiao and Xiaoqun Wang. Conditional quasi-monte carlo methods and dimension reduction for option pricing and hedging with discontinuous functions. *Journal of Computational and Applied Mathematics*, 343:289–308, 2018.

A Prices for different methods for binary option

Method \Steps	2	4	8	16
MISC ($TOl = 5.10^{-1}$)	0.4620	0.4404	0.4299	0.4250

Table 7: Binary option price of the different methods for different number of time steps, without Richardson extrapolation.

Method \Steps	$1-2$	$2-4$	$4-8$	$8-16$
MISC ($TOl = 5.10^{-1}$)	0.4239	0.4188	0.4194	0.4200
MISC ($TOl = 10^{-2}$)	–	0.4192	0.4194	0.4201
MISC ($TOl = 10^{-3}$)	–	–	0.4198	0.4205

Table 8: Binary option price of the different methods for different number of time steps, with Richardson extrapolation (level 1).

B Call prices for different methods

Method \Steps	2	4	8	16
MISC ($TOl = 5.10^{-1}$)	16.2145	16.1352	16.0275	15.9594
MISC ($TOl = 10^{-3}$)	–	16.1328	–	–

Table 9: Call option price of the different methods for different number of time steps, without Richardson extrapolation.

Method \Steps	$1-2$	$2-4$	$4-8$	$8-16$
MISC ($TOl = 5.10^{-1}$)	16.4419	16.0558	15.9205	15.8915
MISC ($TOl = 10^{-3}$)	–	16.0510	15.9177	15.8880

Table 10: Call option price of the different methods for different number of time steps, with Richardson extrapolation (level 1).

Method \Steps	$1-2-4$	$2-4-8$	$4-8-16$
MISC ($TOl = 5.10^{-1}$)	15.9269	15.8756	15.8815
MISC ($TOl = 10^{-3}$)	15.9205	15.8732	15.8789

Table 11: Call option price of the different methods for different number of time steps, with Richardson extrapolation (level 2).